JACS
JOURNAL OF THE AMERICAN CHEMICAL SOCIETY
Article
pubs.acs.org/JACS

Pentameric Circular Iron(II) Double Helicates and a Molecular Pentafoil Knot

Jean-François Ayme,[†] Jonathon E. Beves,[†] David A. Leigh,*[,†,‡] Roy T. McBurney,[†] Kari Rissanen,[¶] and David Schultz[†]

[†]School of Chemistry, University of Edinburgh, The King's Buildings, West Mains Road, Edinburgh EH9 3JJ, United Kingdom
[‡]School of Chemistry, University of Manchester, Oxford Road, Manchester M13 9PL, United Kingdom
[¶]Department of Chemistry, Nanoscience Center, University of Jyväskylä, P.O. Box 35, 40014 JYU, Finland

Supporting Information

ABSTRACT: We report on the synthesis of 11 pentameric cyclic helicates formed by imine condensation of alkyl monoamines with a common bis(formylpyridine)-bipyridyl-derived building block and iron(II) and chloride ions. The cyclic double-stranded helicates were characterized by NMR spectroscopy, mass spectrometry, and in the case of a 2,4-dimethoxybenzylamine-derived pentameric cyclic helicate, X-ray crystallography. The factors influencing the assembly process (reactant stoichiometry, concentration, solvent, nature and amount of anion) were studied in detail: the role of chloride in the assembly process appears not to be limited to that of a simple template, and larger circular helicates observed with related tris(bipyridine) ligands with different iron salts are not produced with the imine ligands. Using certain chiral amines, pentameric cyclic helices of single handedness could be isolated and the stereochemistry of the helix determined by circular dichroism. By employing a particular diamine, a closed-loop molecular pentafoil knot was prepared. The pentafoil knot was characterized by NMR spectroscopy, mass spectrometry, and X-ray crystallography, confirming the topology and providing insights into the reasons for its formation.

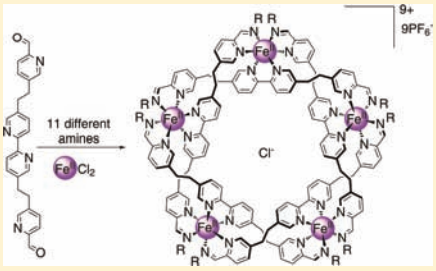

1. INTRODUCTION

The interweaving of molecular strands in DNA,[1] proteins,[2] and natural[3] and synthetic polymers[4] significantly affects their mechanical, physical, and chemical properties. The presence of knots in proteins can increase stability and improve function[5] and has provided insights into the mechanisms of protein folding.[2a,3] Knots have been tied in biopolymers with optical tweezers[6] and can also be formed from surfactant nanotubes[7] and chiral nematic colloids.[8] For synthetic chemists the key challenge in the synthesis of entwined and interlocked molecular structures is the generation and linking (with the correct connectivity) of crossing points.[9] Template and self-assembly methods[9−14]—including the use of metal ions,[9,10] $\pi-\pi$ interactions,[11] hydrogen bonding,[12] hydrophobic interactions,[13] and anions[14]—have proven powerful tools for this task. Sauvage pioneered the use of linear metal helicates[15] to access mechanically interlocked molecules, entwining ligands about one, two, or three tetrahedral copper(I) centers to generate the required crossing points for [2]catenanes,[16] trefoil knots[17] and a Solomon link,[18] respectively. Despite these and other metal template syntheses of trefoil knots[19] and strategies based on hydrogen bonding[20] and $\pi-\pi$ stacking,[21] higher-order non-DNA molecular knots remained elusive until the recently described[22] synthesis of a molecular pentafoil knot, a closed-loop pentameric cyclic Fe(II) double helicate. Here we report on the chemistry behind that synthesis, including the assembly of 11 'open' pentameric cyclic iron(II) double helicates prepared from monoamines, and the use of this framework to form the molecular pentafoil knot. The cyclic helicates are characterized in solution and the solid state, and the factors affecting the assembly process investigated. Both similarities and differences are found between the synthesis of these circular helicates featuring imine bonds and analogous circular helicates derived from tris(bipyridine) ligands.

2. CYCLIC HELICATES AND THEIR POTENTIAL FOR MOLECULAR KNOT SYNTHESIS

Despite the success in using metal helicates to form interlocked molecules with up to four crossing points,[16−18] attempts to generate interlocked structures from longer linear helicates have, to date, proved unsuccessful.[23] This is probably due to the large separation between the end groups of each of the ligand strands disfavoring their reaction to form structures with the required connectivity. Cyclic systems might offer a way of overcoming this problem, since the reactive end-groups can be brought close together in such architectures. The first circular helicates[24] were discovered by Lehn and co-workers,[24a,b,d] who noted their potential for forming complex topologies.[24a] However, multiple coupling reactions would be required to form entwined closed loops, which are inherently more demanding than single ring-closing reactions. The coupling

Received: April 7, 2012
Published: May 3, 2012

   dx.doi.org/10.1021/ja303355v | J. Am. Chem. Soc. 2012, 134, 9488−9497

reactions would need to be functional group specific, high yielding, and ideally, reversible to allow the potential for error correction of wrongly connected strands during the reaction. The conditions (ethylene glycol, 170 °C[24a,b,d]) used to form circular helicates with Lehn's original tris(bipyridine) ligands are not compatible with most types of reactive functional groups.

In recent years, great strides have been made in dynamic covalent chemistry.[25] Reversible imine-bond formation has proven highly effective for linking multiple building blocks in the construction of catenanes,[26] rotaxanes,[27] cages,[28] Solomon links,[29] and Borromean rings.[30] We decided to investigate this method for the formation of cyclic helicates using a ligand inspired by Lehn's original three-bipyridine-strand design,[24a] replacing the two terminal bipyridine units with 2-formylpyridine groups. Reaction of dialdehyde **1** with amines (to form imine groups) would generate a tris(bidentate) ligand strand, which we hoped could be assembled into cyclic double helicate structures with iron(II) ions.

3. RESULTS AND DISCUSSION

Dialdehyde **1** was synthesized from commercially available 5-bromo-2-iodopyridine and 5-bromo-2-formylpyridine via a series of Sonogashira coupling reactions and deprotection steps in 19% overall yield, with six steps in the longest linear sequence (for details, see the Supporting Information [SI]).

Reaction of **1** with 2.2 equiv of 4-methoxylbenzylamine (**2a**) in DMSO-d_6 and 1.1 equiv of anhydrous iron(II) chloride (Scheme 1) immediately gave an intensely colored purple

Scheme 1. Synthesis of Pentameric Cyclic Helicates [3a–k]Cl(PF$_6$)$_9$[a]

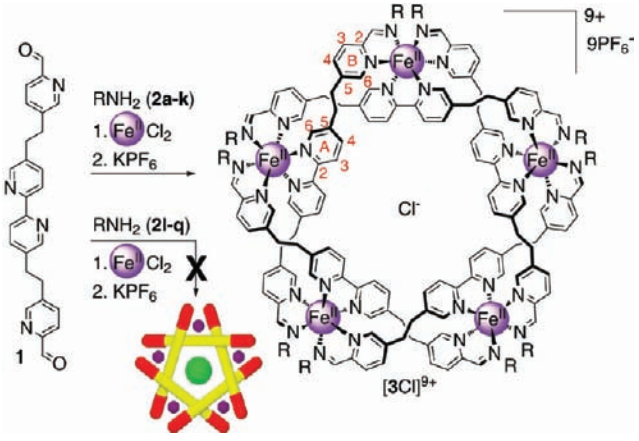

[a]Reaction conditions: 1. Dialdehyde **1**/FeCl$_2$/amine **2a–q** (1:1.1:2.2), DMSO-d_6, 60 °C, 1–2 days. 2. Aqueous KPF$_6$.

solution, typical of low-spin iron(II) tris(diimine) complexes.[31] The ^{1}H NMR spectrum (DMSO-d_6) of the initial reaction mixture contained only broad signals, indicative of the formation of poorly defined oligomeric and polymeric species. However, on heating at 60 °C, the spectrum gradually simplified until after 15 h a single major species was present in solution. Anion exchange was performed using excess aqueous potassium hexafluorophosphate (KPF$_6$) to give a fine purple suspension, which was collected, washed, and dissolved in acetonitrile, to give [**3a**Cl](PF$_6$)$_9$ in 54% isolated yield. Electrospray mass spectrometry (ESI-MS, Figure 1) showed 3+, 4+, 5+, 6+, and 7+ signals with isotope patterns corresponding

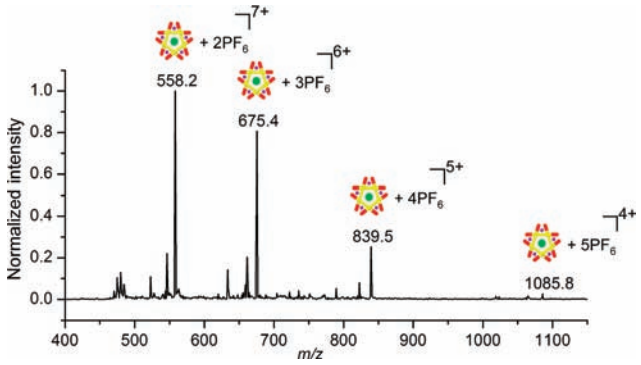

Figure 1. ESI-MS of cyclic helicate [**3a**Cl](PF$_6$)$_9$ showing signals corresponding to sequential loss of PF$_6$ anions. Calculated peaks (*m*/*z*): 558.2 [M-7PF$_6$]$^{7+}$, 675.4 [M-6PF$_6$]$^{6+}$, 839.5 [M-5PF$_6$]$^{5+}$, 1085.8 [M-4PF$_6$]$^{4+}$.

to sequential loss of PF$_6$ anions from a pentameric species containing five ligands, five iron(II) cations, and one chloride anion. No chloride-free species were observed, confirming the binding of a single chloride ion that could not be removed by repeated anion exchange with KPF$_6$.

The ^{1}H NMR spectrum of the isolated product contained only one set of signals for each type of building block (no end-groups, Figure 2e), consistent with a symmetrical cyclic structure. Signals for the py-CH$_2$ and N–CH$_2$ methylene groups appear as diastereotopic pairs which, in combination with the ESI-MS data, confirmed the product to be a chiral (racemic) cyclic helicate [**3a**Cl]$^{9+}$ (Scheme 1). The H^{A3} signal (see Scheme 1 for numbering scheme) is shifted to very low field (9.87 ppm), consistent with strong hydrogen bonding of these protons to the central chloride ion. Having established that the reaction of these building blocks afforded pentameric cyclic helicates, we sought to probe the structural tolerance of the reaction and investigate factors that control the assembly process.

4. STRUCTURAL REQUIREMENTS FOR PENTAMERIC CYCLIC HELICATE ASSEMBLY

The pentameric cyclic helicate assembly process shown in Scheme 1 proved to be very sensitive to the nature of the monoamine building block (Table 1). The effect of having different substituents on benzylamine was profound: electron-withdrawing groups [4-bromo-**2l** (Table 1, entry 12); 3-bromo-**2m** (Table 1, entry 13); 4-trifluoromethyl-**2n**; (Table 1, entry 14)] gave exclusively polymeric or oligomeric products (e.g., Figure 2a). In contrast, the use of electron-rich benzylamine derivatives [4-methoxy-**2a** (Table 1, entry 1); 2,4-dimethoxy-**2b** (Table 1, entry 2)] formed the cyclic helicates in high yields with few byproducts (d and e of Figure 2). Benzylamine itself gave a modest yield (30%) of cyclic helicate (Table 1, entry 4) accompanied by significant amounts of oligomeric byproducts in the crude reaction mixture.

The steric bulk about the amine functional group also significantly influences the outcome of the reaction (Table 1). 3-Phenylpropylamine (**2f**, Table 1, entry 6, 55%) and 4-phenylbutylamine (**2g**, Table 1, entry 7, 52%) resulted in higher cyclic helicate yields than the more hindered 2-phenylethylamine (**2e**, Table 1, entry 5, 43%). The use of anilines (**2o**, Table 1, entry 15) or sterically hindered amines (**2p** and **2q**, Table 1, entries 16 and 17) initially gave intensely purple-colored solutions apparently consisting of polymeric species

dx.doi.org/10.1021/ja303355v | J. Am. Chem. Soc. 2012, 134, 9488–9497

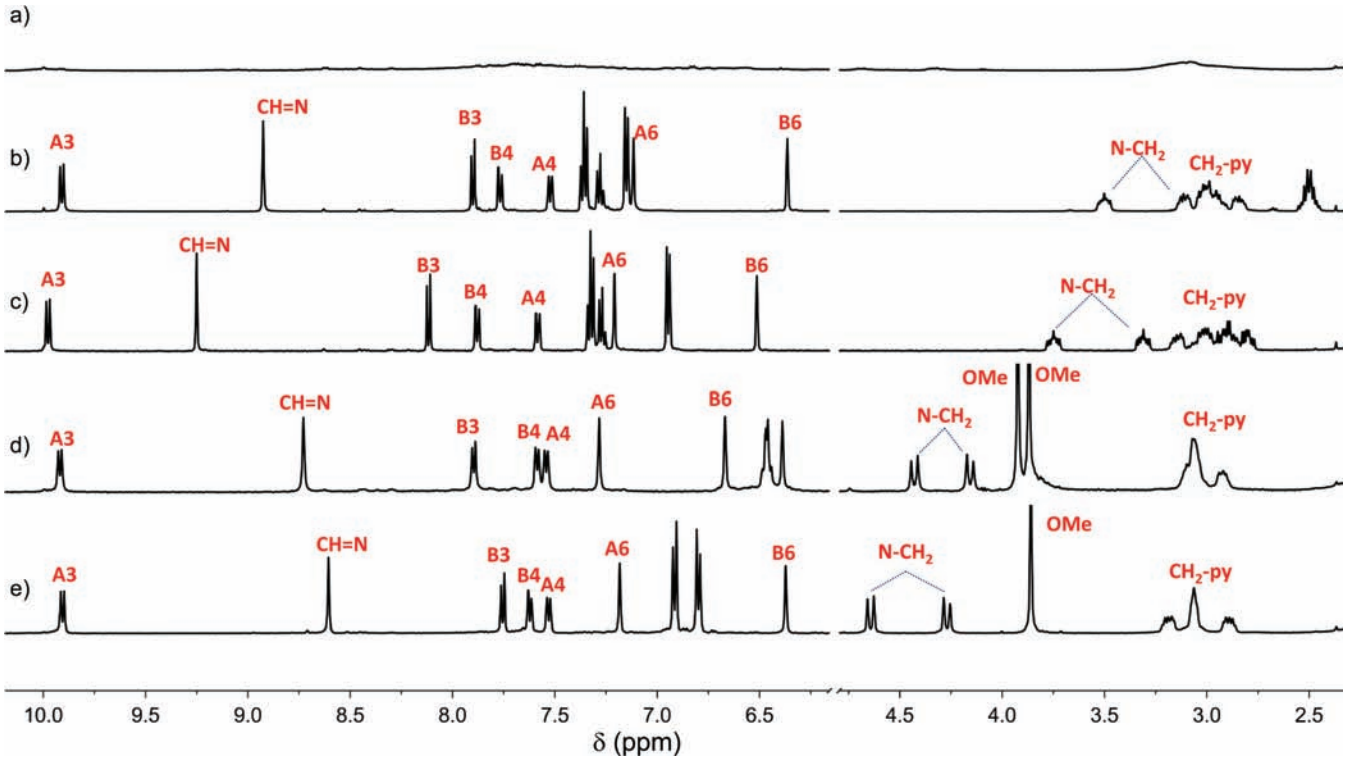

Figure 2. ^{1}H NMR (CD_3CN, 500 MHz, 298 K) of the products isolated from the reaction of dialdehyde **1** and various amines (**2l**, **2f**, **2e**, **2b**, and **2a**) in the presence of $FeCl_2$ (Scheme 1). (a) Amine used 4-bromobenzylamine (**2l**; Table 1, entry 12). The broad ^{1}H NMR spectrum is characteristic of polymers. (b) [**3f**Cl]$(PF_6)_9$. (c) [**3e**Cl]$(PF_6)_9$. (d) [**3b**Cl]$(PF_6)_9$. (e) [**3a**Cl]$(PF_6)_9$. All samples were colored purple of similar intensities. The assignments correspond to the labeling shown in Scheme 1.

(broad ^{1}H NMR spectra). However, upon being heated, pale-orange high-spin iron(II) complexes were formed, with no ESI-MS evidence for the formation of short linear or cyclic helicates. Sterically unhindered aliphatic primary amines (e.g., hexylamine **2h** and dodecylamine **2i**, Table 1, entries 8 and 9) gave the highest yields of cyclic helicates (63% for [**3h**Cl]-$(PF_6)_9$) and the fewest byproducts.

5. PROBING THE REACTION CONDITIONS OF PENTAMERIC CYCLIC HELICATE ASSEMBLY

Various factors (reagent stoichiometry, influence of various anions, the role of chloride, the effect of solvent, concentration, and preforming the diimine ligand) influencing the outcome of the pentameric cyclic helicate-forming reaction shown in Scheme 1 were investigated, mainly through a series of studies using hexylamine (**2h**) as the amine (Scheme 2).

5.1. Reactant Stoichiometry. Reactant stoichiometry proved to be extremely important, with a ratio of 1:1.1:2.2 dialdehyde **1**/$FeCl_2$/**2h** giving 63% of cyclic helicate [**3h**]Cl-$(PF_6)_9$ (Table 1, entry 8). The use of less than 2 equiv of amine **2h** (with respect to **1**) gave mixtures of products, including $[Fe(\mathbf{1})_3]^{6+}$ and related species (see SI, Figure S10). Substoichiometric amounts of $FeCl_2$ (with respect to **1**) gave low yields of circular helicate and complex mixtures of products (SI, Figure S9). Although employing an excess of amine also resulted in a substantial decrease in yield (SI, Figure S10), the lack of other high-molecular weight byproducts meant that the cyclic helicate products were most easily isolated using these conditions. Somewhat surprisingly, the use of excess $FeCl_2$ gave the highest yields of cyclic helicate with 1.5, 2.2, and 4.4 equiv of $FeCl_2$ (with respect to **1**) giving 84, 85, and 91% yields of [**3h**Cl]$(PF_6)_9$, respectively (Figure 3).

5.2. Influence of Anions. The substitution of $FeCl_2$ for other iron(II) salts [$Fe(SO_4)_2{\cdot}7H_2O$, $Fe(CH_3CO_2)_2$, $Fe(BF_4)_2{\cdot}6H_2O$, $Fe(ClO_4)_2{\cdot}6H_2O$, $Fe(ClO_4)_2{\cdot}xH_2O$] in the reactions shown in Scheme 1 invariably gave complex mixtures with no ESI-MS evidence for the formation of circular helicates of any size, in contrast to the cyclic hexameric helicate reported by Lehn using his related tris(bipyridine) ligand with $Fe(BF_4)_2{\cdot}6H_2O$ or $FeBr_2$.[24b] However, when 4-methylbenzylamine (**2c**) was employed with iron(II) tetrafluoroborate [$Fe(BF_4)_2{\cdot}6H_2O$] or iron(II) perchlorate [$Fe(ClO_4)_2{\cdot}6H_2O$] a discrete low-molecular weight product was formed in under 10% yield; no related products were observed with hexylamine (**2h**) or other aliphatic amines. ESI-MS evidence supported the assignment of this minor product as the linear trinuclear triple-stranded helicate[24a] $[Fe_3L_3]^{6+}$ (see SI, page S22).

5.3. Role of Chloride Ions. The role of chloride in the pentameric cyclic helicate forming reaction shown in Scheme 2 was investigated using varying amounts of $Fe(BF_4)_2{\cdot}6H_2O$ and $FeCl_2$ in order to vary the amount of chloride present in the reaction while maintaining a constant iron(II) concentration (Figure 4, blue data points). The yield of the isolated cyclic pentameric helicate $[\mathbf{3h}Cl]^{9+}$ increased steeply with the amount of chloride, up to 0.4 chloride ions per iron(II) (i.e., approximately two chloride ions per cyclic helicate, 44% yield), and then increased less sharply as the amount of chloride increased further up to 63% with 2.0 Cl^- per Fe(II).

Similar results were obtained using $Fe(BF_4)_2{\cdot}6H_2O$ as the sole iron(II) source and adding tetrabutylammonium chloride[32] (Figure 4, red data points, and SI, Figure S15). Under these conditions chloride/iron(II) ratios greater than 2:1 could be

dx.doi.org/10.1021/ja303355v | J. Am. Chem. Soc. 2012, 134, 9488−9497

Table 1. Yields of Pentameric Cyclic Helicates from the Reaction Shown in Scheme 1 with Monoamines 2a–q[a]

Entry		Amine	Helicate $[FeL_5Cl](PF_6)_9$	Isolated yield (%)
1	**2a**	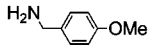	**[3a**Cl](PF$_6$)$_9$	54
2	**2b**	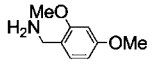	**[3b**Cl](PF$_6$)$_9$	48
3	**2c**	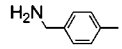	**[3c**Cl](PF$_6$)$_9$	52
4	**2d**	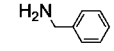	**[3d**Cl](PF$_6$)$_9$	30
5	**2e**	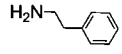	**[3e**Cl](PF$_6$)$_9$	43
6	**2f**	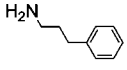	**[3f**Cl](PF$_6$)$_9$	55
7	**2g**	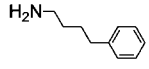	**[3g**Cl](PF$_6$)$_9$	52
8	**2h**		**[3h**Cl](PF$_6$)$_9$	63
9	**2i**		**[3i**Cl](PF$_6$)$_9$	53[b]
10	**2j**	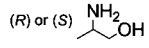	**[3j**Cl](PF$_6$)$_9$	34
11	**2k**	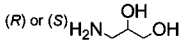	**[3k**Cl](PF$_6$)$_9$	46[c]
12	**2l**	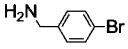	-	-[d]
13	**2m**	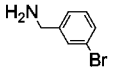	-	-[d]
14	**2n**	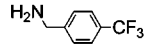	-	-[e]
15	**2o**	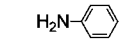	-	-[e]
16	**2p**	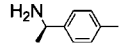	-	-[f]
17	**2q**	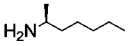	-	-[f]

[a]Reaction conditions: 1.1:1.1:2.2 of **1**/$FeCl_2$/amine, DMSO-d_6, 60 °C, 1 d (except entry 10, 2 d). 2. Aqueous KPF_6. [b]Reaction performed in 1:1 $CDCl_3/CD_3CN$ due to the poor solubility of **2i** in DMSO. [c]Yield of major diastereoisomer. [d]Intensely colored purple solutions with only broad ^{1}H NMR signals, likely polymeric materials. [e]Initially gave an intensely colored purple solution, which became pale yellow upon heating overnight. [f]Pale-yellow/orange solutions, assumed to be high-spin iron(II) complexes, with no ESI-MS evidence for cyclic helicate formation.

obtained, which resulted in slight decreases in yield (e.g., 4:1 Cl/Fe gave 60% yield of [**3h**Cl]$^{9+}$). Interestingly, the use of higher ratios with respect to **1** of both Fe(II) and Cl^- resulted in significant increases in yield. For example, where 4.4 equiv of $Fe(BF_4)_2{\cdot}6H_2O$ was used (with respect to **1**) the yield of [**3h**Cl]$^{9+}$ increased linearly with chloride concentration, with 90% yield being obtained where 4 equiv of chloride (with respect to dialdehyde **1**) was added (Figure 4, black data points). A similar yield was obtained where 4.4 equiv of $FeCl_2$ was used (see section 5.1, Reactant Stoichiometry).

The pentameric cyclic helicates bind Cl^- ions extremely strongly ($K_a > 10^{10}$ M^{-1}) in a 1:1 complex.[22a] The finding that one equivalent of chloride is not generally sufficient to effectively template the formation of the circular pentameric helicates at millimolar concentrations appears to rule out a simple thermodynamic template effect[33,9] and indicates that the

Scheme 2. Synthesis of Pentameric Cyclic Helicate [3h]Cl(PF$_6$)$_9$ from Dialdehyde 1 and Hexylamine (2h) or Preformed Diimine Ligand 4[a]

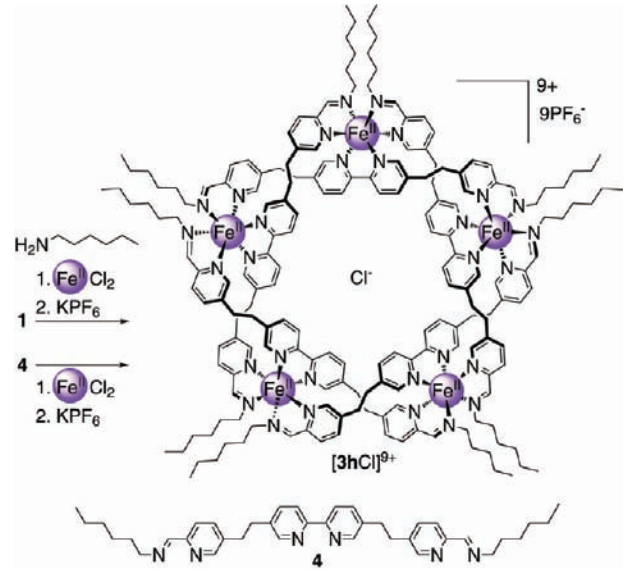

[a]Reaction conditions: 1. Dialdehyde **1**/$FeCl_2$/**2h** (1:1.1:2.2) or **4**/$FeCl_2$ (1:1.1), DMSO-d_6, 60 °C, 1 day. 2. Aqueous KPF_6.

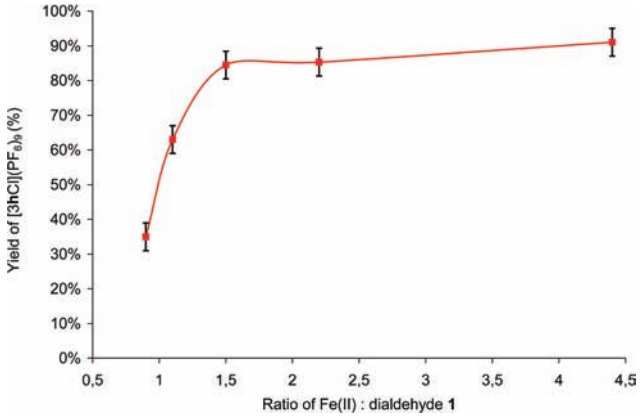

Figure 3. Influence of $FeCl_2$/dialdehyde **1** ratio [2.2 equiv of hexylamine (**2h**)] on the yield of [**3h**Cl](PF$_6$)$_9$. Error bars ±5%.

chloride ions play a more complicated role in the assembly process. It seems likely that they aid the rearrangement of oligomers in the reaction mixture until the stable chloride-binding pentameric cyclic helicate is formed.[34]

5.4. Solvent and Concentration. DMSO proved to be the solvent of choice for the pentameric cyclic helicate-forming reactions for most amines, with methanol, ethanol, nitromethane, acetonitrile, diglyme ($MeOCH_2CH_2OMe$), and mixtures of these solvents with halogenated solvents either giving precipitates or pale-yellow solutions indicative of high-spin iron(II) complexes. Dodecylamine (**2i**) proved an exception,[35] with helicate [**3i**Cl]$^{9+}$ being formed in good yield in acetonitrile–chloroform (1:1) solution (Table 1, entry 9), presumably due to the solubilizing effect of the long alkyl chains. Generally, heating the reaction mixtures at higher temperatures (e.g., 100 °C in DMSO) resulted in discoloration over several hours, indicating decomposition of the putative Fe(II)–diimine complexes.[36] Reaction concentration is also important,[24b] with relatively high initial concentrations of

dx.doi.org/10.1021/ja303355v | J. Am. Chem. Soc. 2012, 134, 9488–9497

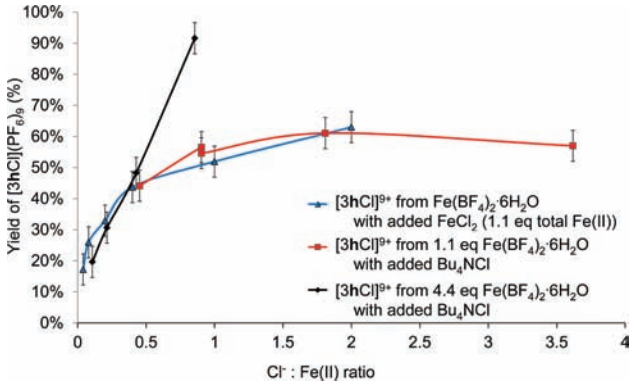

Figure 4. Effect of chloride ions on the yield of helicate $[\mathbf{3h}Cl]^{9+}$. The reactions were carried out using mixtures of either $Fe(BF_4)_2{\cdot}6H_2O$ and $FeCl_2$ (blue data points), or $Fe(BF_4)_2{\cdot}6H_2O$ and tetrabutylammonium chloride (red data points = 1.1 equiv of Fe(II); black data points = 4.4 total equiv of Fe(II)), with Bu_4NBF_4 added to maintain a constant Bu_4N^+ concentration. In all cases the ratio of dialdehyde (**1**)/hexylamine (**2h**) was 1:1.1. The highest yield, 90%, was obtained using 4.4 equiv of $Fe(BF_4)_2{\cdot}6H_2O$ (with respect to dialdehyde **1**) with 4 equiv of Bu_4NCl (i.e., 0.9 equiv of Cl^- per Fe(II); black line). Error bars ±5%. See SI, Figure S14.

reactants (~5 mM) delivering the highest yields of pentameric cyclic helicate products. Very dilute reaction conditions (<0.01 mM) gave low yields of circular helicates.

5.5. Rate of Pentameric Circular Helicate Formation. The rate of formation of pentameric cyclic helicate $[\mathbf{3h}Cl]^{9+}$ (Scheme 2) was followed by ^{1}H NMR spectroscopy (Figure 5,

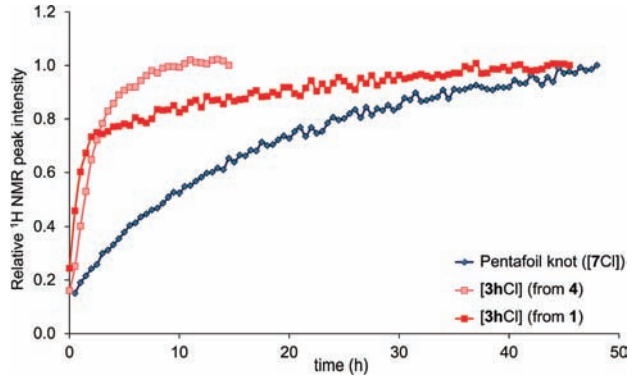

Figure 5. Rate of formation of pentameric cyclic helicate $[\mathbf{3h}Cl]^{9+}$ (Scheme 2) from dialdehyde **1** and hexylamine (**2h**) (pink squares) or from preformed ligand **4** (red squares). The rate of formation of pentafoil knot $[7Cl]^{9+}$ from dialdehyde **1** and diamine **6** (Scheme 3) is also shown (blue diamonds). The reactions were maintained at 60 °C and ^{1}H NMR spectra collected (600 MHz, DMSO-d_6) every 30 min. Relative peak integral of imine peak shown, normalized to the integral of the final time-point in each case. See SI, Figures S7 and S8.

red data points). Under the standard reaction conditions (**1**/$FeCl_2$/**2h** (1:1.1:2.2), DMSO-d_6, 60 °C) the reaction was essentially complete after 24 h (after which time there was little change in the ^{1}H NMR spectrum). In order to simplify the study of the assembly process, ligand **4** was prepared to both eliminate initial imine formation from the reaction kinetics and to allow a strict 1:1 ratio of amine/aldehyde to be employed (see SI, Figure S7).

When employing **4** instead of **1** and **2h** in the reaction shown in Scheme 2, the rate of pentameric cyclic helicate ($[\mathbf{3h}Cl]^{9+}$) formation was more rapid (Figure 5, pink data points), although some imine hydrolysis was also observed. A comparison of the rate of formation of $[\mathbf{3h}Cl]^{9+}$ when starting from **4** or **1**/**2h** confirms that metal–ligand exchange is likely the rate-limiting factor in the rearrangement of rapidly formed simple complexes (e.g., $Fe_3(\mathbf{4})_3$ and related species), oligomers, and polymers into the pentameric cyclic helicate.

6. X-RAY CRYSTAL STRUCTURE OF PENTAMERIC CYCLIC HELICATE [3BCL](PF$_6$)$_9$

Purple crystals of pentameric circular helicate $[\mathbf{3b}Cl](PF_6)_9$ suitable for single-crystal X-ray diffraction were grown by slow diffusion of diethyl ether vapor into a solution of the complex in nitromethane–acetonitrile. The structure crystallized in the $P2_1/c$ space group with the asymmetric unit containing a single pentameric cyclic helicate (Figure 6).[37] The five iron(II)

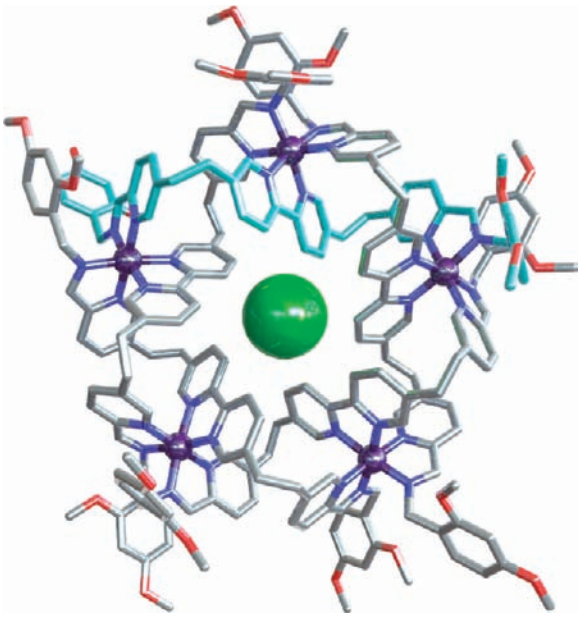

Figure 6. X-ray crystal structure of $[\mathbf{3b}Cl](PF_6)_9{\cdot}x$solvent, from a single crystal obtained by vapor diffusion of diethyl ether into a acetonitrile–nitromethane solution.[37] Anions, solvent molecules, and hydrogen atoms are omitted for clarity. Nitrogen atoms are shown in dark blue, oxygen atoms red, chlorine atom green, and carbon atoms gray; the carbon framework of a single ligand is colored light blue. Fe(II) centers shown at 50% van der Waals radius, Cl^- shown at 100%. $Cl^-\cdots$HC distances (clockwise from top-left blue bipyridine unit): 2.75, 2.68, 2.69, 2.81, 2.78, 2.68, 2.71, 2.71, 2.73, 2.78 Å. C–H–Cl angles (deg) 176.3, 177.5, 175.5, 176.7, 178.4, 175.8, 178.1, 179.4, 174.0, 176.8. For packing diagrams, see SI, Figures S24 and S25.

centers lie in a near-perfect plane (maximum displacement of a Fe(II) from the least-squares plane is 0.091(1) Å). The coordination geometry of the iron(II) ions shows Fe–N and N–Fe–N bond lengths and angles at the limits of normal ranges and, as for Lehn's pentameric cyclic helicate,[24a] the overall geometries of the metal centers are among the most distorted for $[Fe(pyridine)_6]$ structures in the Cambridge Structural Database (CSD) (see SI). The chloride ion is in close contact with the 10 H^{A3} protons ($Cl^-\cdots H^{A3}C$ distances 2.679(1)–2.814(1) Å) and displaced from the least-squares plane defined by the five Fe(II) centers by 1.475(1) Å, indicating that the symmetry of the solution ^{1}H NMR spectrum must result from oscillation of the anion between the two sides

dx.doi.org/10.1021/ja303355v | J. Am. Chem. Soc. 2012, 134, 9488–9497

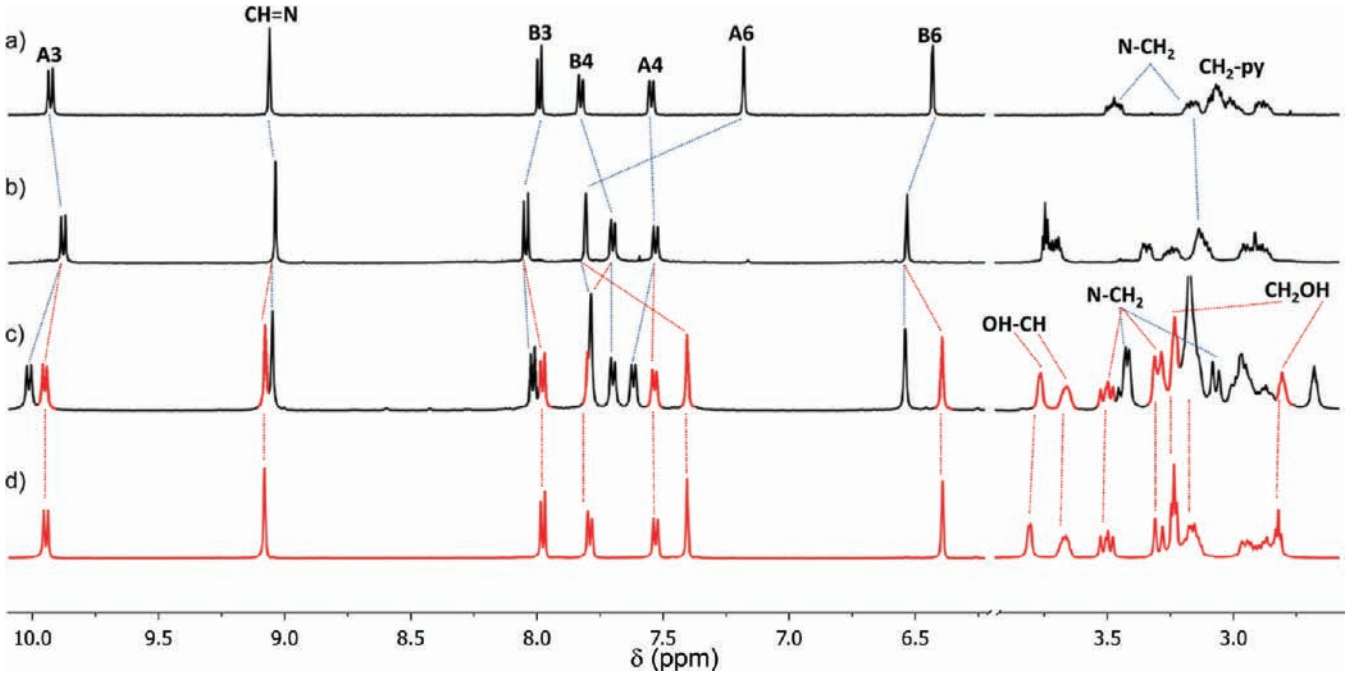

Figure 7. ^{1}H NMR (500 MHz, CD_3CN, 298 K) of pentameric cyclic helicates derived from (a) hexylamine ([**3h**Cl]$(PF_6)_9$), (b) diastereoselective helicate [**3j**Cl]$(PF_6)_9$, (c) mixture of diastereomers formed with (*R*)-amino-2,3-propandiol (**2k**) (This spectrum is after partial workup and has been enriched in the minor diastereomer. The crude reaction mixture shows a ∼1:2 ratio of diastereomers.), and (d) isolated major diastereoisomer ([**3k**Cl]$(PF_6)_9$) from (*R*)-amino-2,3-propandiol (**2k**). The assignments correspond to the labeling shown in Scheme 1.

of the circular helicate that is fast on the NMR time scale. The phenyl rings adopt a range of orientations, engaging in weak $\pi-\pi$ stacking interactions to form zigzag 2D sheets of helicates in the *ab*-plane (see SI), with weaker interactions between these sheets.

7. CONTROLING THE HELIX STEREOCHEMISTRY OF PENTAMERIC CYCLIC HELICATES

We next focused on attempting to form pentameric cyclic helicates of single handedness. Many examples of stereochemical control of linear helicate formation have been reported,[38] and one example of a single-stranded circular helicate,[38d] usually by employing chiral auxiliaries covalently attached to the ends of the ligands or by incorporating chiral structures such as BINOL (1,1′-bi-2-naphthol) or *trans*-1,2-diaminocyclohexane into the center regions of the ligands. The aldehyde groups at either end of building block **1** enables the straightforward preparation of enantiopure ligands by condensation reactions with appropriate chiral amines.[38m]

Initially, we investigated chiral derivatives closely related to those of monoamines found to form pentameric cyclic helicates in reasonable yields, i.e. amines **2p** and **2q** (Table 1, entries 16 and 17). Disappointingly, however, both amines generated only pale yellow reaction mixtures (indicative of high-spin iron(II) complexes) and no discrete complexes could be isolated following anion exchange. This also proved to be the case for a range of other chiral α-substituted amines (see SI, Figure S5). We speculated that the methyl group adjacent to the amine might be too sterically demanding to allow helicate formation (see section 4, Structural Requirements for Pentameric Cyclic Helicate Assembly) and tried a primary amine with a chiral hydroxyl group two atoms away from the amine center ((*R*)-**2k**). This formed both diastereoisomers of pentameric cyclic helicate [**3k**Cl]$^{9+}$ with ∼1:2 diastereoselectivity (Table 1, entry 11, and Figure 7c). The major diastereomer was isolated in 46% yield by recrystallization from acetonitrile−water (the minor diastereoisomer has significantly higher solubility).

Finally, in contrast to the unsuccessful reactions with other α-substituted primary amines (Table 1, entries 16 and 17, and SI, Figure S5), enantiopure (*R*)- or (*S*)-2-amino-1-propanol (**2j**) generated pentameric cyclic helicate [**3j**Cl]$^{9+}$ with complete diastereoselectivity (the enantiomers of the amine-producing pentameric cyclic helicates of opposite helix stereochemistry), in isolated yields of 32%. The ^{1}H NMR spectra showed a large and unexpected peak shift for the H^{A6} signal, shifted downfield by 0.63 ppm relative to the equivalent signal of helicate [**3h**Cl]$(PF_6)_9$. A ROESY NMR spectrum was consistent with the presence of a CH···O hydrogen bond between the OH group and H^{A6} of the bipyridine unit (SI, Figure S18) which likely plays a significant stabilizing role in formation of the pentameric cyclic helicate from this hindered amine.

The helix stereochemistry of the pentameric cyclic helicates formed from the chiral amines was investigated by circular dichroism (CD). The UV−visible absorption spectrum of helicate [**3j**Cl]$(PF_6)_9$ is shown in Figure 8 and is representative of helicates [**3a**−**k**Cl]$(PF_6)_9$. An intense and broad MLCT transition is centered at 566 nm, with a shoulder at higher energy (centered at 520 nm)[39] and a strong $\pi-\pi^*$ transition at 310 nm, typical of low-spin [Fe(diimine)$_3$]$^{2+}$ complexes. The CD spectra of (*R*)-[**3j**Cl]$(PF_6)_9$ and (*S*)-[**3j**Cl]$(PF_6)_9$ are shown in Figure 8 and are qualitatively similar to those of related systems.[40] The interpretation of CD spectra of octahedral coordination complexes has been shown to be a reliable means of assigning absolute stereochemistry of M(N^N)$_3$ (N^N = 2,2′-bipyridine, 1,10-phenanthroline)-type complexes using exciton theory.[41] Using this method, the CD spectra of [(*R*)-**3j**Cl]$^{9+}$ and [(*S*)-**3j**Cl]$^{9+}$ were assigned as ΔΔΔΔΔ-[**3j**Cl]$^{9+}$ and ΛΛΛΛΛ-[**3j**Cl]$^{9+}$, respectively, in

dx.doi.org/10.1021/ja303355v | *J. Am. Chem. Soc.* 2012, 134, 9488−9497

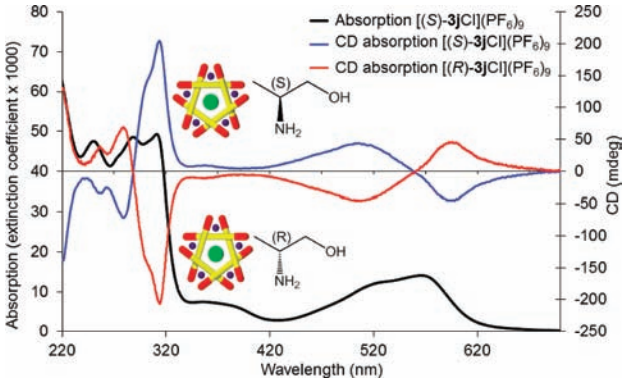

Figure 8. UV−vis absorption (black, left axis) and circular dichroism of pentameric cyclic helicates $[(R)\text{-}\mathbf{3j}\mathrm{Cl}](\mathrm{PF_6})_9$ and $[(S)\text{-}\mathbf{3j}\mathrm{Cl}](\mathrm{PF_6})_9$ in CH_3CN (0.12 mM).

agreement with related assignments (SI, pages S38−S40).[42] The isolated major diastereomer $[(R)\text{-}\mathbf{3k}\mathrm{Cl}]^{9+}$ has a CD spectrum similar to that of $[(S)\text{-}\mathbf{3j}\mathrm{Cl}]^{9+}$, corresponding to ΛΛΛΛΛ-$[\mathbf{3k}\mathrm{Cl}]^{9+}$, and in agreement with NMR ROESY data (SI, Figure S18).

8. ASSEMBLY OF A MOLECULAR PENTAFOIL KNOT

Having established that nonhindered, aliphatic monoamines formed pentameric circular helicates in the highest yields with the fewest byproducts, we reasoned that the use of alkyl diamines could allow the formation of a molecular pentafoil knot (Scheme 3).[22] Somewhat unexpectedly, the use of C_6−C_{12}

Scheme 3. Synthesis of Molecular Pentafoil Knot $[\mathbf{7}\mathrm{Cl}](\mathrm{PF_6})_9$.[a]

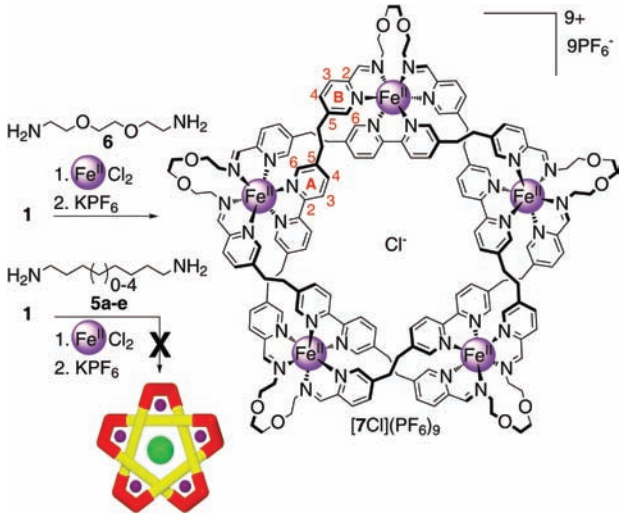

[a]Reaction conditions: 1. Dialdehyde **1**/$FeCl_2$/diamine **6** (1:1.1:2.2), DMSO-d_6, 60 °C, 2 days. 2. Aqueous KPF_6. 44% yield $[\mathbf{7}\mathrm{Cl}](\mathrm{PF_6})_9$. The use of diamines **5a−e** instead of **6** did not generate the corresponding pentafoil knots.

diaminoalkanes (**5a−e**) gave only intractable material, with no evidence for the formation of the desired knots. Similarly, diamines based on bridged 4-(alkoxy)benzylamines gave only oligomeric/polymeric products (see SI, Figure S5). When employing a glycol linker, 2,2′-(ethylenedioxy)bis(ethylamine) (**6**), the reaction mixture also initially gave a featureless ^{1}H NMR spectrum (Figure 9e). However, on heating at 60 °C, the

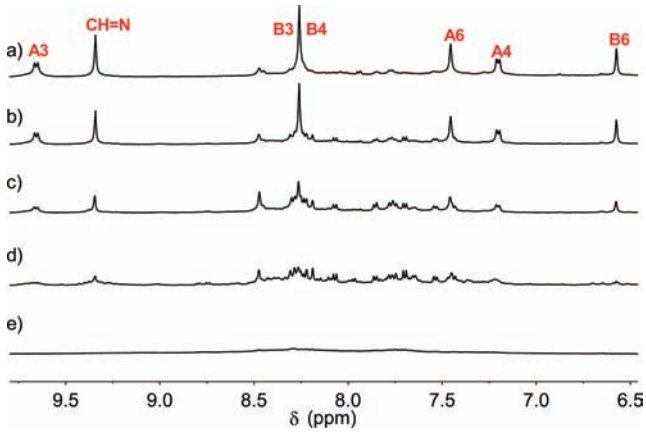

Figure 9. ^{1}H NMR spectra (DMSO-d_6, 500 MHz, 298 K) of the formation of pentafoil knot $[\mathbf{7}\mathrm{Cl}]^{9+}$ (Scheme 3). Reaction mixture after (e) 5 min, (d) 2 h, (c) 10 h, (b) 26 h, and (a) 48 h at 60 °C. The assignments correspond to the labeling shown in Scheme 3.

mixture slowly rearranged over two days to form a single major species (Figure 9a). Aspects of the ^{1}H NMR spectrum are very similar to that of the hexylamine derivative $[\mathbf{3h}\mathrm{Cl}](\mathrm{PF_6})_9$, suggesting that these two compounds have closely related structures. After workup, the molecular pentafoil knot $[\mathbf{7}\mathrm{Cl}](\mathrm{PF_6})_9$ was isolated in 44% yield and its structure confirmed by ESI-MS (see SI, page S21).[22]

Some aspects of the assembly of the open cyclic helicates $[\mathbf{3a}\text{−}\mathbf{k}\mathrm{Cl}]^{9+}$ translate poorly to the pentafoil knot $[\mathbf{7}\mathrm{Cl}]^{9+}$ assembly process. First, the rate of formation of the knot is significantly slower than that of the open cyclic helicates (Figure 5), indicating that interconversions and rearrangements of the intermediates are slower with the diamine. Second, the stoichiometry of reagents proved to be more critical for the pentafoil knot than for the open circular helicate systems. The use of increasing amounts of $FeCl_2$ relative to dialdehyde **1** resulted in lower yields (e.g., the use of 2 equiv of $FeCl_2$ with respect to dialdehyde **1** resulted in a 40% drop in yield relative to when 1.1 equiv of $FeCl_2$ was used; SI, Figure S12). This is in contrast with the findings for the open systems where increased ratios of $FeCl_2$ substantially increased yields (see section 5.1. Reactant Stoichiometry). The use of excess diamine in the knot-forming reaction resulted in even more severe reductions in yield (e.g., 2.0 equiv of diamine **6** resulted in a 90% fall in relative yield, SI, Figure S11). Finally, the reaction also proved very sensitive to the ratio of $FeCl_2$/amine employed, with a 1:1 ratio giving the highest yields (SI, Figure S13). As with the open systems, the formation of pentafoil knot $[\mathbf{7}\mathrm{Cl}]^{9+}$ was sensitive to the amount of chloride present, with the yield increasing to a maximum with a ratio of 2:1 chloride/iron(II) (SI, Figure S15). The requirement for more than one Cl^- ion per molecular pentafoil knot despite very strong knot/chloride 1:1 binding[22] suggests that the role of Cl^- in the assembly process is more complicated than just as a simple template. Higher amounts of chloride ion in the reaction did not increase the yield of pentafoil knot further (SI, Figures S15 and S16).

Purple crystals of pentafoil knot $[\mathbf{7}\mathrm{Cl}](\mathrm{PF_6})_9 \cdot x(\text{solvent})$ were grown by slow diffusion of diethyl ether vapor into an acetonitrile−toluene (3:2) solution of the complex and the X-ray structure determined using diffraction data collected on beamline I19 at the Diamond Light Source (U.K.).[22] The solid state structure (Figure 10) confirmed the topology of the pentafoil knot. As for the open cyclic helicate $[\mathbf{3b}\mathrm{Cl}](\mathrm{PF_6})_9$

dx.doi.org/10.1021/ja303355v | J. Am. Chem. Soc. 2012, 134, 9488−9497

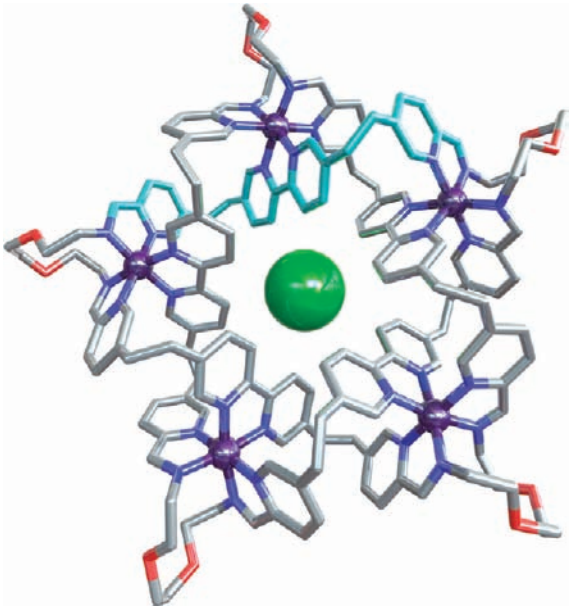

Figure 10. X-ray crystal structure of pentafoil knot $[7Cl](PF_6)_9$, from a single crystal obtained by vapor diffusion of diethyl ether into a acetonitrile–toluene solution.[22] Hexafluorophosphate anions, solvent molecules, and hydrogen atoms are omitted for clarity. Nitrogen atoms are shown in dark blue, oxygen atoms red, chlorine atom green, and carbon atoms gray (the carbon framework originating from a single building block of **1** is colored light blue). Fe(II) centers shown at 50% van der Waals radius, Cl^- shown at 100%. Cl···HC distances (clockwise from top left blue bipyridine unit): 2.71, 2.75, 2.76, 2.70, 2.76, 2.70, 2.69, 2.71, 2.71, 2.69. C–H–Cl– angles (deg): 172, 179, 170, 176, 172, 177, 176, 176, 170, 178. For an ORTEP plot, see the SI, Figure S26.

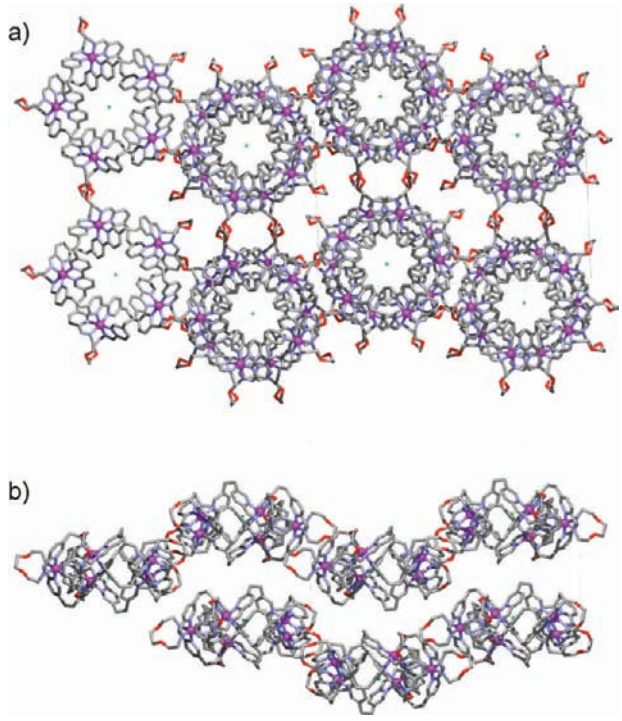

Figure 11. Crystal packing diagrams for the X-ray structure of $[7Cl](PF_6)_9 \cdot x$solvent viewed down (a) the crystallographic *c*-axis and (b) the crystallographic *a*-axis. Close contacts between glycol chains dominate the intermolecular contacts, forming 2D sheets of the molecular knots that are separated by disordered solvent and anions (omitted for clarity).

(Figure 6), the structure contains a single helicate in the asymmetric unit and crystallizes in the $P2_1/c$ space group. The planar geometry of the iron centers and the displacement of the chloride ion from this plane are similar to that in $[\mathbf{3b}Cl]^{9+}$. Eight of the nine PF_6 anions are located in the difference map, and the structure also contains disordered solvent molecules. The structure is generally well-ordered (see SI, Figure S26, for ORTEP plot), with the exception of the glycol linkers which show large thermal displacement parameters. The glycol chains have O–C–C–O torsion angles ranging from 57(3)° to 77(2)°. It seems likely that the gauche effect[43] (the preference for O–C–C–O chains to adopt torsion angles of 60° rather than the 180° angle of all-carbon chains) stabilizes this low-energy turn which is likely responsible for diamine **6** forming the closed-loop pentafoil knot, whereas other diaminoalkanes of similar length (**5a–e**) do not (Scheme 3).[44] The molecules are packed in 2D zigzag arrays, with close contacts between the glycol linkers (CH···HC contacts as short as 2.22 Å, Figure 11).

9. CONCLUSIONS

Pentameric cyclic double helicates can be efficiently assembled in a one-pot reaction from iron(II) cations, dialdehyde **1**, and a range of monoamines (**2a–k**) in the presence of chloride anions. The assembly process is very sensitive to the structure of the amine, reactant stoichiometry (dialdehyde/Fe(II)/amine:Cl^-) and reaction conditions (solvent, concentration). Some of the ways that these factors influence the assembly process are somewhat unexpected:

The reagent stoichiometry that corresponds to the composition of the pentameric circular helicate products [5:5:10:1 dialdehyde/Fe(II)/amine/Cl^-] does not give the highest yield. Rather the use of significant excesses of iron(II) and chloride ions give the highest (virtually quantitative) yields of open circular helicates, indicating that these ions likely play more important roles in the assembly process than that of a simple thermodynamic template.

Due to the symmetry of the cyclic helicate structure, the effect of individually rather weak interactions on the assembly process is magnified, and can significantly alter the product distribution in the reaction mixture. In some cases this can be beneficial (for example, to form cyclic helicates of specific handedness with particular chiral amines) and in others detrimental (for example, sterically hindered amines favoring polymer formation over circular helicates).

The subtle effects of structure on the assembly reaction is also illustrated by the fact that circular helices other than the pentamer are not observed in the reaction of **1** with amines and different iron(II) salts. This contrasts with the formation of hexameric circular helicates with Lehn's tris(bipyridine) ligands and $Fe(BF_4)_2 \cdot 6H_2O$ or $FeBr_2$.[24b]

By using a diamine that can form a low-energy turn due to the gauche effect on its glycol linkers the assembly system was successfully used to form a molecular pentafoil knot.[22] The reagent stoichiometry effects observed for open circular helicate formation do not all translate to the pentafoil knot. For example, the use of an increased amount of iron(II) with respect to **1** lowered the yield of the knot, the opposite of that found for the open circular helicates.

dx.doi.org/10.1021/ja303355v | J. Am. Chem. Soc. 2012, 134, 9488–9497

The use of cyclic helicates as scaffolds for the assembly of interlocked molecules builds upon, and complements, the linear helicate strategy introduced by Sauvage in the 1980s.[10] We anticipate that the information gleaned from the investigation of the assembly processes presented here will be useful for the rational synthesis of higher-order topologically complex molecular architectures.

■ ASSOCIATED CONTENT

Supporting Information

Experimental procedures and spectral data for all compounds and the details of the X-ray analyses of [**3b**Cl]$(PF_6)_9$·*x*solvent and [7Cl]$(PF_6)_9$·*x*solvent including CIF files. This material is available free of charge via the Internet at http://pubs.acs.org.

■ AUTHOR INFORMATION

Corresponding Author

David.Leigh@manchester.ac.uk

Notes

The authors declare no competing financial interest.

■ ACKNOWLEDGMENTS

We thank the Diamond Light Source (U.K.) for synchrotron beamtime on I19 (XR029), the Engineering and Physical Sciences Research Council (EPSRC) National Crystallography Service for data collection, and the EPSRC National Mass Spectrometry Service Centre (Swansea, U.K.) for high-resolution mass spectrometry. J.E.B. and D.S. are Swiss National Science Foundation postdoctoral fellows. This research was funded by the EPSRC and the Academy of Finland (K.R., Projects 212588 and 218325). We thank Robert W. McGregor (www.mcgregorfineart.com) for the images of the X-ray crystal structures.

■ REFERENCES

(1) (a) Wasserman, S. A.; Cozzarelli, N. R. *Science* **1986**, *232*, 951–960. (b) Du, S. M.; Seeman, N. C. *J. Am. Chem. Soc.* **1992**, *114*, 9652–9655. (c) Du, S. M.; Stollar, B. D.; Seeman, N. C. *J. Am. Chem. Soc.* **1995**, *117*, 1194–1200.

(2) (a) Taylor, W. R. *Nature* **2000**, *406*, 916–919. (b) King, N. P.; Jacobitz, A. W.; Sawaya, M. R.; Goldschmidt, L.; Yeates, T. O. *Proc. Natl. Acad. Sci. U.S.A.* **2010**, *107*, 20732–20737.

(3) (a) Andersson, F. I.; Pina, D. G.; Mallam, A. L.; Blaser, G.; Jackson, S. E. *FEBS* **2009**, *276*, 2625–2635. (b) Mallam, A. L.; Rogers, J. M.; Jackson, S. E. *Proc. Natl. Acad. Sci. U.S.A.* **2010**, *107*, 8189–8194. (c) Meluzzi, D.; Smith, D. E.; Arya, G. *Annu. Rev. Biophys.* **2010**, *39*, 349–366.

(4) (a) Saitta, A. M.; Soper, P. D.; Wasserman, E.; Klein, M. L. *Nature* **1999**, *399*, 46–48. (b) Virnau, P.; Kantor, Y.; Kardar, M. *J. Am. Chem. Soc.* **2005**, *127*, 15102–15106.

(5) Belmonte, A. *Proc. Natl. Acad. Sci. U.S.A.* **2007**, *104*, 17243–17244.

(6) Arai, Y.; Yasuda, R.; Akashi, K.-I.; Harada, Y.; Miyata, H.; Kinosita, K., Jr.; Itoh, H. *Nature* **1999**, *399*, 446–448.

(7) Lobovkina, T.; Dommersnes, P.; Joanny, J.-F.; Bassereau, P.; Karlsson, M.; Orwar, O. *Proc. Natl. Acad. Sci. U.S.A.* **2004**, *101*, 7949–7953.

(8) Tkalec, U.; Ravnik, M.; Čopar, S.; Žumer, S.; Muševič, I. *Science* **2011**, *333*, 62–65.

(9) Beves, J. E.; Blight, B. A.; Campbell, C. J.; Leigh, D. A.; McBurney, R. T. *Angew. Chem., Int. Ed.* **2011**, *50*, 9260–9327.

(10) (a) Chambron, J.-C.; Dietrich-Buchecker, C.; Sauvage, J.-P. In *Comprehensive Supramolecular Chemistry*; Sauvage, J.-P., Hosseini, M. W., Eds.; Elsevier: Oxford, 1996; Vol. *9*, pp 43–83; (b) Hubin, T. J.; Busch, D. H. *Coord. Chem. Rev.* **2000**, *200*, 5–52. (c) Collin, J.-P.; Dietrich-Buchecker, C.; Hamann, C.; Jouvenot, D.; Kern, J.-M.; Mobian, P.; Sauvage, J.-P. In *Comprehensive Coordination Chemistry II*; McCleverty, J. A., Meyer, T. J., Eds.; Elsevier: Amsterdam, 2004; Vol. *7*, pp 303–326.

(11) (a) Loeb, S. J. *Chem. Soc. Rev.* **2007**, *36*, 226–235. (b) Griffiths, K. E.; Stoddart, J. F. *Pure Appl. Chem.* **2008**, *80*, 485–506.

(12) (a) Cantrill, S. J.; Pease, A. R.; Stoddart, J. F. *J. Chem. Soc., Dalton Trans.* **2000**, 3715–3734. (b) Kay, E. R.; Leigh, D. A. *Top. Curr. Chem.* **2005**, *262*, 133–177.

(13) (a) Fujita, M. *Acc. Chem. Res.* **1999**, *32*, 53–61. (b) Frampton, M. J.; Anderson, H. L. *Angew. Chem., Int. Ed.* **2007**, *46*, 1028–1064.

(14) Mullen, K. M.; Beer, P. D. *Chem. Soc. Rev.* **2009**, *38*, 1701–1713.

(15) Albrecht, M. *Top. Curr. Chem.* **2004**, *248*, 105–139.

(16) Dietrich-Buchecker, C. O.; Sauvage, J.-P.; Kintzinger, J.-P. *Tetrahedron Lett.* **1983**, *24*, 5095–5098.

(17) (a) Dietrich-Buchecker, C. O.; Sauvage, J.-P. *Angew. Chem., Int. Ed. Engl.* **1989**, *28*, 189–192. (b) Rapenne, G.; Dietrich-Buchecker, C.; Sauvage, J.-P. *J. Am. Chem. Soc.* **1996**, *118*, 10932–10933. (c) Meyer, M.; Albrecht-Gary, A.-M.; Dietrich-Buchecker, C. O.; Sauvage, J.-P. *J. Am. Chem. Soc.* **1997**, *119*, 4599–4607.

(18) Nierengarten, J. F.; Dietrich-Buchecker, C. O.; Sauvage, J. P. *J. Am. Chem. Soc.* **1994**, *116*, 375–376.

(19) (a) Rapenne, G.; Dietrich-Buchecker, C.; Sauvage, J.-P. *J. Am. Chem. Soc.* **1999**, *121*, 994–1001. (b) Adams, H.; Ashworth, E.; Breault, G. A.; Guo, J.; Hunter, C. A.; Mayers, P. C. *Nature* **2001**, *411*, 763–763. (c) Guo, J.; Mayers, P. C.; Breault, G. A.; Hunter, C. A. *Nature Chem.* **2010**, *2*, 218–222. (d) Barran, P. E.; Cole, H. L.; Goldup, S. M.; Leigh, D. A.; McGonigal, P. R.; Symes, M. D.; Wu, J.; Zengerle, M. *Angew. Chem., Int. Ed.* **2011**, *50*, 12280–12284.

(20) (a) Safarowsky, O.; Nieger, M.; Fröhlich, R.; Vögtle, F. *Angew. Chem., Int. Ed.* **2000**, *39*, 1616–1618. (b) Vögtle, F.; Hunten, A.; Vogel, E.; Buschbeck, S.; Safarowsky, O.; Recker, J.; Parham, A.-H.; Knott, M.; Muller, W. M.; Muller, U.; Okamoto, Y.; Kubota, T.; Lindner, W.; Francotte, E.; Grimme, S. *Angew. Chem., Int. Ed.* **2001**, *40*, 2468–2471. (c) Lukin, O.; Kubota, T.; Okamoto, Y.; Kaufmann, A.; Vögtle, F. *Chem.—Eur. J.* **2004**, *10*, 2804–2810. (d) Lukin, O.; Vögtle, F. *Angew. Chem., Int. Ed.* **2005**, *44*, 1456–1477. (e) Feigel, M.; Ladberg, R.; Engels; Herbst-Irmer, R.; Fröhlich, R. *Angew. Chem., Int. Ed.* **2006**, *45*, 5698–5702. (f) Passaniti, P.; Ceroni, P.; Balzani, V.; Lukin, O.; Yoneva, A.; Vögtle, F. *Chem.—Eur. J.* **2006**, *12*, 5685–5690. (g) Brüggemann, J.; Bitter, S.; Müller, S.; Müller, W. M.; Müller, U.; Maier, N. M.; Lindner, W.; Vögtle, F. *Angew. Chem., Int. Ed.* **2007**, *46*, 254–259.

(21) Ashton, P. R.; Matthews, O. A.; Menzer, S.; Raymo, F. M.; Spencer, N.; Stoddart, J. F.; Williams, D. J. *Liebigs Ann./Recl.* **1997**, 2485–2494.

(22) (a) Ayme, J.-A.; Beves, J. E.; Leigh, D. A.; McBurney, R. T.; Rissanen, K.; Schultz, D. *Nature Chem.* **2012**, *4*, 15–20. (b) Hardie, M. J. *Nature Chem.* **2012**, *4*, 7–8.

(23) Dietrich-Buchecker, C.; Colasson, B.; Jouvenot, D.; Sauvage, J.-P. *Chem.—Eur. J.* **2005**, *11*, 4374–4386.

(24) (a) Hasenknopf, B.; Lehn, J.-M.; Kneisel, B. O.; Baum, G.; Fenske, D. *Angew. Chem., Int. Ed. Engl.* **1996**, *35*, 1838–1840. (b) Hasenknopf, B.; Lehn, J.-M.; Boumediene, N.; Dupont-Gervais, A.; Van Dorsselaer, A.; Kneisel, B.; Fenske, D. *J. Am. Chem. Soc.* **1997**, *119*, 10956–10962. (c) Provent, C.; Hewage, S.; Brand, G.; Bernardinelli, G.; Charbonnière, L. J.; Williams, A. F. *Angew. Chem., Int. Ed. Engl.* **1997**, *36*, 1287–1289. (d) Hasenknopf, B.; Lehn, J.-M.; Boumediene, N.; Leize, E.; Van Dorsselaer, A. *Angew. Chem., Int. Ed.* **1998**, *37*, 3265–3268. (e) Provent, C.; Rivara-Minten, E.; Hewage, S.; Brunner, G.; Williams, A. F. *Chem.—Eur. J.* **1999**, *5*, 3487–3494. (f) Childs, L. J.; Alcock, N. W.; Hannon, M. J. *Angew. Chem., Int. Ed.* **2002**, *41*, 4244–4247. (g) Tuna, F.; Hamblin, J.; Jackson, A.; Clarkson, G.; Alcock, N. W.; Hannon, M. J. *Dalton Trans.* **2003**, 2141–2148. (h) Childs, L. J.; Pascu, M.; Clarke, A. J.; Alcock, N. W.; Hannon, M. J. *Chem.—Eur. J.* **2004**, *10*, 4291–4300. (i) Senegas, J.-M.; Koeller, S.; Bernardinelli, G.; Piguet, C. *Chem. Commun.* **2005**, 2235–2237. (j) Hamblin, J.; Tuna, F.; Bunce, S.; Childs, L. J.; Jackson, A.; Errington, W.; Alcock, N. W.; Nierengarten, H.; Van Dorsselaer,

A.; Leize-Wagner, E.; Hannon, M. J. *Chem.—Eur. J.* **2007**, *13*, 9286–9296. (k) Pang, Y.; Cui, S.; Li, B.; Zhang, J.; Wang, Y.; Zhang, H. *Inorg. Chem.* **2008**, *47*, 10317–10324. (l) Allen, K. E.; Faulkner, R. A.; Harding, L. P.; Rice, C. R.; Riis-Johannessen, T.; Voss, M. L.; Whitehead, M. *Angew. Chem., Int. Ed.* **2010**, *49*, 6655–6658. (m) Bain, L.; Bullock, S.; Harding, L.; Riis-Johannessen, T.; Midgley, G.; Rice Craig, R.; Whitehead, M. *Chem. Commun.* **2010**, *46*, 3496–3498. (n) Tanh Jeazet, H. B.; Gloe, K.; Doert, T.; Kataeva, O. N.; Jäger, A.; Geipel, G.; Bernhard, G.; Büchner, B.; Gloe, K. *Chem. Commun.* **2010**, *46*, 2373–2375. (o) Giles, I. D.; Chifotides, H. T.; Shatruk, M.; Dunbar, K. R. *Chem. Commun.* **2011**, *47*, 12604–12606.

(25) (a) Corbett, P. T.; Leclaire, J.; Vial, L.; West, K. R.; Wietor, J.-L.; Sanders, J. K. M.; Otto, S. *Chem. Rev.* **2006**, *106*, 3652–3711. (b) Lehn, J.-M. *Chem. Soc. Rev.* **2007**, *36*, 151–160.

(26) (a) Leigh, D. A.; Lusby, P. J.; Teat, S. J.; Wilson, A. J.; Wong, J. K. Y. *Angew. Chem., Int. Ed.* **2001**, *40*, 1538–1543. (b) Price, J. R.; Clegg, J. K.; Fenton, R. R.; Lindoy, L. F.; McMurtrie, J. C.; Meehan, G. V.; Parkin, A.; Perkins, D.; Turner, P. *Aust. J. Chem.* **2009**, *62*, 1014–1019.

(27) Hogg, L.; Leigh, D. A.; Lusby, P. J.; Morelli, A.; Parsons, S.; Wong, J. K. Y. *Angew. Chem., Int. Ed.* **2004**, *43*, 1218–1221.

(28) Hutin, M.; Frantz, R.; Nitschke, J. R. *Chem.—Eur. J.* **2006**, *12*, 4077–4082.

(29) Pentecost, C. D.; Chichak, K. S.; Peters, A. J.; Cave, G. W. V.; Cantrill, S. J.; Stoddart, J. F. *Angew. Chem., Int. Ed.* **2007**, *46*, 218–222.

(30) Chichak, K. S.; Cantrill, S. J.; Pease, A. R.; Chiu, S.-H.; Cave, G. W. V.; Atwood, J. L.; Stoddart, J. F. *Science* **2004**, *304*, 1308–1312.

(31) Twigg, M. V.; Burgess, J. In *Comprehensive Coordination Chemistry II*; McCleverty, J. A., Meyer, T. J., Eds.; Elsevier: Amsterdam, 2004; Vol. *5*, pp 403–553.

(32) Bu_4NBF_4 was also added to maintain a constant Bu_4N^+ concentration.

(33) Thompson, M. C.; Busch, D. H. *J. Am. Chem. Soc.* **1964**, *86*, 213–217.

(34) Chloride ions have been previously shown to catalyze the rate of ligand exchange of $[Fe(phen)_3]^{2+}$ complexes in DMSO, see Farrinton, D. J.; Jones, J. O.; Twigg, M. V. *Inorg. Chim. Acta* **1977**, *25*, L75–L76.

(35) This is likely primarily a solubility issue: in order for the kinetic distribution of oligomers which are initially formed to rearrange into the thermodynamically preferred product, these must all remain in solution at all times. Dodecylamine (which is not soluble in DMSO) affords the circular helicate increased solubility in chloroform (by comparison with circular helicates $[\mathbf{3a}–\mathbf{3g}]^{10+}$) and allows the rearrangement process to proceed readily.

(36) The isolated pentameric circular helicates were found to be stable in MeCN at 60 °C for several weeks, with no evidence for decomposition. However, the addition of a monoamine to isolated samples of the circular helicates resulted only in the decomposition of the helicate, with little evidence for amine exchange. Attempts were made to reduce the imine groups of the molecular pentafoil knot $[\mathbf{7Cl}](PF_6)_9$ using standard procedures ($NaBH_4$), but these resulted in decomplexation, and no organic knot could be isolated from the reaction mixture.

(37) Crystal data for $[\mathbf{3b}Cl](PF_6)_9 \cdot x$solvent: purple blocks, 0.11 mm × 0.15 mm × 0.32 mm, M = 5358.62, $C_{240}H_{234}ClF_{45}N_{37}O_{20}P_{7.5}Fe_5$, monoclinic, space group $P2_1/c$, a = 34.023(2) Å, b = 23.714(2) Å, c = 36.537(2) Å, β = 94.386(2)°, V = 29393(4) Å^3, Z = 4, D_c = 1.211 g/cm^3, 3211 parameters, 151 restraints, R = 0.1388 [$I_o > 2\sigma(I_o)$], wR = 0.3829 (all reflections).

(38) (a) Zarges, W.; Hall, J.; Lehn, J. M.; Bolm, C. *Helv. Chim. Acta* **1991**, *74*, 1843–1852. (b) Constable, E. C.; Kulke, T.; Baum, G.; Fenske, D. *Chem. Commun.* **1997**, 2043–2044. (c) Constable, E. C.; Kulke, T.; Baum, G.; Fenske, D. *Inorg. Chem. Commun.* **1998**, *1*, 80–82. (d) Mamula, O.; von Zelewsky, A.; Bernardinelli, G. *Angew. Chem., Int. Ed.* **1998**, *37*, 290–293. (e) Baum, G.; Constable, E. C.; Fenske, D.; Housecroft, C. E.; Kulke, T. *Chem.—Eur. J.* **1999**, *5*, 1862–1873. (f) Lutzen, A.; Hapke, M.; Griep-Raming, J.; Haase, D.; Saak, W. *Angew. Chem., Int. Ed.* **2002**, *41*, 2086–2089. (g) Orita, A.; Nakano, T.; An, D. L.; Tanikawa, K.; Wakamatsu, K.; Otera, J. *J. Am. Chem. Soc.* **2004**, *126*, 10389–10396. (h) Wood, T. E.; Dalgleish, N. D.; Power, E. D.; Thompson, A.; Chen, X.; Okamoto, Y. *J. Am. Chem. Soc.* **2005**, *127*, 5740–5741. (i) Kreickmann, T.; Diedrich, C.; Pape, T.; Huynh, H. V.; Grimme, S.; Hahn, F. E. *J. Am. Chem. Soc.* **2006**, *128*, 11808–11819. (j) Bunzen, J.; Bruhn, T.; Bringmann, G.; Lützen, A. *J. Am. Chem. Soc.* **2009**, *131*, 3621–3630. (k) Stomeo, F.; Lincheneau, C.; Leonard, J. P.; O'Brien, J. E.; Peacock, R. D.; McCoy, C. P.; Gunnlaugsson, T. *J. Am. Chem. Soc.* **2009**, *131*, 9636–9637. (l) Amendola, V.; Boiocchi, M.; Brega, V.; Fabbrizzi, L.; Mosca, L. *Inorg. Chem.* **2010**, *49*, 997–1007. (m) Howson, S. E.; Bolhuis, A.; Brabec, V.; Clarkson, G. J.; Malina, J.; Rodger, A.; Scott, P. *Nature Chem.* **2012**, *4*, 31–36.

(39) (a) This is typical for Fe(diimine)$_3$ complexes. It is known that the isomeric forms of these complexes have practically identical absorption spectra [Krumholz, P. *Inorg. Chem.*, **1965**, 609], and that the energy of the MLCT is strongly influenced by the number of coordinated aromatic rings [(b) Busch, D. H.; Bailar, J. C., Jr. *J. Am. Chem. Soc.* **1956**, *78*, 1137–1142]. For example, MLCT in water: Fe(Me-N=CH–CH=N-Me)$_3$ 568 nm,[39b] [Fe(py-CH=NH–CH_3)$_3$]I_2 551 nm,[39b] and [Fe(py-CH=NH–CH_3)$_3$]$(ClO_4)_2$ 551 nm.[39a] As the number of coordinated aromatic rings increases, the energy of the MLCT increases, with $[Fe(bpy)_3]^{2+}$ and $[Fe(phen)_3]^{2+}$ exhibiting λ_{max} at 490 and 510 nm, respectively. Combined, these data surprisingly suggest that the the ligands in the present helicates behave less like aromatic ligands such as bipyridine and more like nonaromatic diimines.

(40) (a) Mürner, H.; von Zelewsky, A.; Hopfgartner, G. *Inorg. Chim. Acta* **1998**, *271*, 36–39. (b) Kiehne, U.; Lützen, A. *Org. Lett.* **2007**, *9*, 5333–5336. (c) Howson, S. E.; Allan, L. E. N.; Chmel, N. P.; Clarkson, G. J.; van Gorkum, R.; Scott, P. *Chem. Commun.* **2009**, 1727–1729.

(41) (a) Bosnich, B. *Acc. Chem. Res.* **1969**, *2*, 266–273. (b) Mason, S. F. *Pure Appl. Chem.* **1970**, *24*, 335–359. (c) Ziegler, M.; von Zelewsky, A. *Coord. Chem. Rev.* **1998**, *177*, 257–300.

(42) This is in agreement with both previous simple pyridyl–imine complexes[40c] and a triple-stranded dinuclear Fe(II)-containing helicate. (a) Mürner, H.; von Zelewsky, A.; Hopfgartner, G. *Inorg. Chim. Acta* **1998**, *271*, 36–39. Additionally, the CD band for the MLCT transition of (*S*)-$[\mathbf{3j}Cl](PF_6)_9$ also corresponds to that of Λ-$[Fe(bpy)_3]$: (b) Mason, S. F.; Peart, B. J. *J. Chem. Soc., Dalton Trans.* **1973**, 949–955 (ref 41c) and Λ-$[Ru(phen)_3]$ (ref 41a).

(43) Wolfe, S. *Acc. Chem. Res.* **1972**, *5*, 102–111.

(44) We reasoned that a more rigid and preorganized diamine based on the same glycol linker, but with an aromatic ring at the center in place of an ethyl spacer, may generate the corresponding pentafoil knot in higher yield. However, we found that diamine 2,2′-(1,2-bisoxyphenylene)diethanamine gave exclusively polymeric material, with no evidence for pentamer formation.